IEEE Photonics Journal
An IEEE Photonics Society Publication

All-Optical Actively Mode-Locked Fiber Laser at 2-μm Based on Interband Modulation

Volume 9, Number 5, October 2017

Xu Wu
Zhichao Wu
Tianye Huang
Bingwei Chen
Kaixuan Ren
Songnian Fu

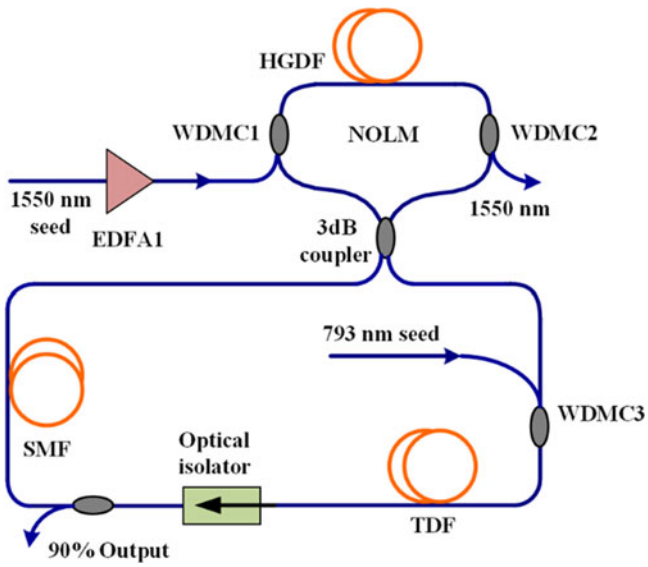

DOI: 10.1109/JPHOT.2017.2756643
1943-0655 © 2017 IEEE

All-Optical Actively Mode-Locked Fiber Laser at 2-μm Based on Interband Modulation

Xu Wu,[1] Zhichao Wu,[2] Tianye Huang [1],[1] Bingwei Chen,[1] Kaixuan Ren,[1] and Songnian Fu[2]

[1]School of Mechanical Engineering and Electronic Information, China University of Geosciences (Wuhan), Wuhan 430074, China
[2]National Engineering Laboratory of Next Generation Internet Access Networks, School of Optical and Electronic Information, Huazhong University of Science and Technology, Wuhan 430073, China

DOI:10.1109/JPHOT.2017.2756643

Manuscript received June 26, 2017; revised August 22, 2017; accepted September 21, 2017. Date of publication September 26, 2017; date of current version October 6, 2017. This work was supported in part by the National Natural Science Foundation of China (61605179), in part by the Fundamental Research Funds for the Central Universities, China University of Geosciences (Wuhan) (162301132703 and G1323511665), and in part by the 863 High Technology Plan (2015AA015502). Corresponding author: Tianye Huang (e-mail: tianye_huang@163.com).

Abstract: In this paper, we have achieved a high repetition rate and tunable pulse generation near ~2 μm through an all-optical actively mode-locked fiber laser. The performances of the fiber laser have been systematically investigated through numerical simulations. The thulium-doped fiber laser cavity is modulated by the optical injection at 1.55 μm via a nonlinear optical loop mirror in which a specially-designed group-velocity-matching highly nonlinear fiber is incorporated. According to the simulation results, up to 40-GHz pulse train with picosecond tunable pulse width and peak power can be produced. Moreover, the repetition rate can be further enlarged with the help of higher gain. The impacts of gain coefficient, cavity length, and repetition rate on the output are studied in details. The proposed mode-locked fiber laser can be potentially used for future 2-μm fiber communication.

Index Terms: Fiber lasers, mode-locked lasers, nonlinear, pulse propagation.

1. Introduction

In the past few years, 2-μm lasers have attracted significant research interests due to their wide applications in the fields of spectroscopy, eye-safe LIDAR, material processing, etc. Since the gain can be provided by thulium-doped fiber (TDF) in this band, various 2-μm fiber lasers have been comprehensively investigated such as high power [1], [2], mode-locked [3], Q-switched [4], wavelength tunable [5], [6], supercontinuum [7], and multiwavelength [8], [9]. More specifically, it should be mentioned that benefitting from the broad gain window of TDF, 2-μm band has also shown great potential to fulfill the requirements of future high data rate and high capacity fiber telecommunication link [10]–[12]. Pulsed laser source with high repetition rate is one of the key modules for both conventional and future fiber communication system such as Nyquist optical time division multiplexing (OTDM) [13]. Therefore, it is foreseeable that there will be great demand for high repetition rate laser sources at 2 μm.

One of the commonly-used approaches for pulse generation is the passively mode-locked fiber laser. However, due to the limited fiber cavity length, it is still challenging to achieve tens of gigahertz level since most of the passively mode-locked lasers operate at the fundamental frequency. Although there are several other techniques, such as passively harmonic mode-locking that can be used to further push the repetition rate [14]–[16], the required higher pump power and critical operation condition may lead to the damage of optical components and the reduction of stability. On the other hand, the operation mechanism of the passively mode-locked fiber laser strongly depends on the interactions of dispersion and nonlinearity arising in the fiber cavity. It is known that those parameters are not easy to adjust during laser emission. Therefore, to achieve the flexible tuning of the repetition rate and pulse width according to different applications is difficult and usually needs complex configuration designs.

In order to achieve laser output with high repetition rate together with tunable capability, actively mode-locked lasers which can synchronize with external source could be a potential choice. As for actively mode-locked fiber lasers, electro-optic modulators can be used to periodically manipulate the attenuation within the cavity and lead to mode-locking. However, the cost of 2-μm band electro-optic modulator is high and the modulation speed is limited [17]. To address those issues, all-optical modulation with $\sim$fs response time in optical fiber is a promising approach [18]. In order to build up an actively mode-locked fiber laser with all-optical modulation, optical pump source with high repetition rate is compulsory. However, at 2 μm, it is still difficult to obtain such pump source. Fortunately, promoted by the development of fiber optical communication, high repetition rate pulse source at 1.55-μm band has come to mature. Therefore, mode-locking a 2 μm fiber laser by using 1.55 μm pump laser can be an alternative approach.

In this paper, an actively mode-locked thulium-doped fiber laser based on inter-band modulation is proposed and numerically investigated. In order to achieve efficient modulation, a highly nonlinear fiber with characteristics of polarization-maintaining and group-velocity-matching between 2 μm and 1.55 μm is firstly designed. Then this fiber is employed to realize a nonlinear optical loop mirror (NOLM) in order to provide intensity modulation within the laser cavity. Through all-optical inter-band modulation, thulium-doped mode-locked fiber laser with tunable output pulse width and repetition rate is demonstrated.

2. Fiber Design for Mode-Locking

In order to efficient modulate the thulium-doped fiber laser by pulse injection, the fiber must possess sufficiently high nonlinearity and the group velocity of the pump pulse ($\sim$1.55 μm) and oscillation pulse ($\sim$2 μm) must be matched. Moreover, in order to improve the stability, the laser cavity is expected to be polarization-maintaining.

Highly germania-doped fiber (HGDF) with a germania-silica core and a silica cladding has attracted extensive interests in the past years, especially at longer wavelength e.g., $\sim$2 μm [19]–[21]. This is because, on one hand, compared with pure silica, the absorption of bulk GeO_2 is smaller near 2 μm. On the other hand, the high nonlinearity of GeO_2 makes HGDF a good platform for nonlinear optics. Here, in order to efficiently modulate the laser cavity by using 1.55-μm pulse train, we design a polarization-maintaining HGDF with group-velocity- matching between 1.55 μm and 2 μm band.

The geometry of the proposed HGDF is shown in Fig. 1(a). The fiber is composed by an elliptical core and a circular cladding with a diameter of $\sim$62.5 μm. The doping concentration of the core region is 70 mol. %. Based on the Sellmeier functions for GeO_2-SiO_2 glasses [22], we can carry out simulation by using COMSOL Multiphysics to calculate the mode properties of such fiber with parameters optimization.

Under conditions of long axis $a = 3$ μm and short axis $b = 2.3$ μm, the mode profiles of TE mode and TM mode at 1550 nm are shown in Fig. 1(b) and (c), respectively. The effective index difference of two linear polarization modes is 8.657×10^{-4}, indicating of good polarization-maintaining property. Particularly, for TM mode, its group velocity in terms of the first-order-dispersion β_1 and dispersion characteristics are demonstrated in Fig. 2(a) and (b), respectively. It can be found that, for TM

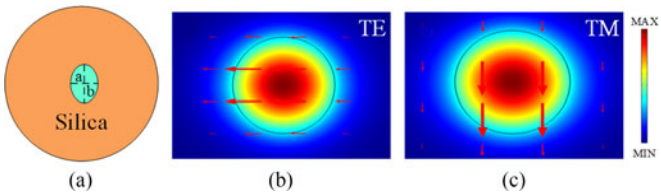

Fig. 1. (a) Schematic diagram of the HGDF, (b) profile of TE mode, and (c) profile of TM-mode.

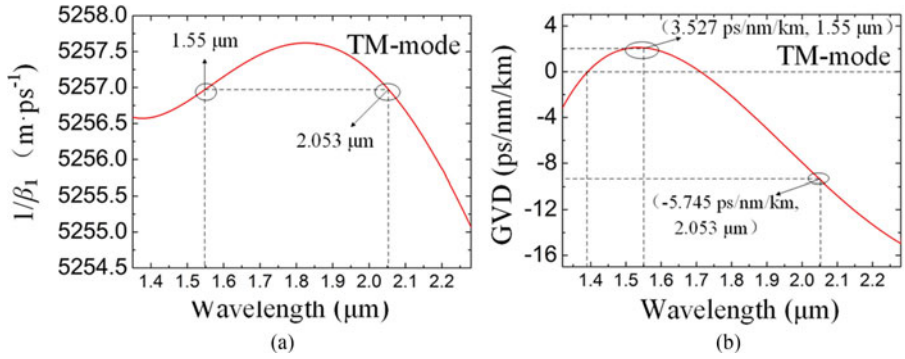

Fig. 2. (a) Group velocity, and (b) group velocity dispersion of HGDF with long axis 3-μm, short axis 2.3-μm.

mode, the group velocities at 1.55 μm and 2.053 μm are equal, leading to the avoidance of walking-off effect during inter-band modulation. The group velocity dispersion GVD possesses small negative value (-5.745 ps/nm/km) at 2 μm indicating normal dispersion. For the nonlinear refractive index of GeO_2-doped silica, a linear relation with silica of $n^{(2)} = (0.0552conc + 2.44) \times 10^{-20}\,m^2/W$ is used to roughly estimate nonlinear refractive index of core and cladding, respectively, where *conc* is the mole concentration. Based on this relation, a nonlinear coefficient of $\sim 27.3\,W^{-1}km^{-1}$ which is nearly 30 times higher than that of conventional SMF can be achieved.

3. Laser Configuration and Numerical Modeling

The actively mode-locking TDF laser with all-optical intensity modulation by a NOLM configuration is schematically shown in Fig. 3. All the fiber and optical components are equipped with polarization-maintaining fiber.

The NOLM with incorporation with the designed HGDF is based on cross-phase modulation (XPM) arising in a Sagnac interferometer. The 1550-nm pump light is coupled into the fiber via a 1550/2000 wavelength division multiplexing coupler (WDMC) to modulate the fiber cavity loss. A section of TDF is used as gain medium, while the single mode fiber (SMF) is used for adjusting the total dispersion of the cavity. An isolator ensures the unidirectional operation. A 90:10 optical coupler (OC) is employed to extract the output pulse at 2 μm.

In numerical model, the propagation of the optical pulse in TDF is governed by Ginzburg-Landau equation as follow [23]:

$$\frac{\partial A}{\partial z} + \frac{\alpha}{2}A + \frac{i}{2}(\beta_2 + ig_0(T_2)^2)\frac{\partial^2 A}{\partial t^2} = i\gamma|A|^2A + \frac{1}{2}g_0A \tag{1}$$

where A is the slowly varying amplitude of the optical pulse envelope, z is the propagation distance through the fiber, β_2 is the second-order dispersion coefficient, γ is the nonlinear coefficient. T_2 is the relaxation time, which is expressed by $T_2 = 1/\triangle\omega$, where $\triangle\omega$ represents the gain bandwidth of TDF, denoted by $\triangle\omega = 2\pi c\triangle\lambda/\lambda^2$, where c is the speed of light in vacuum, $\triangle\lambda$ means the

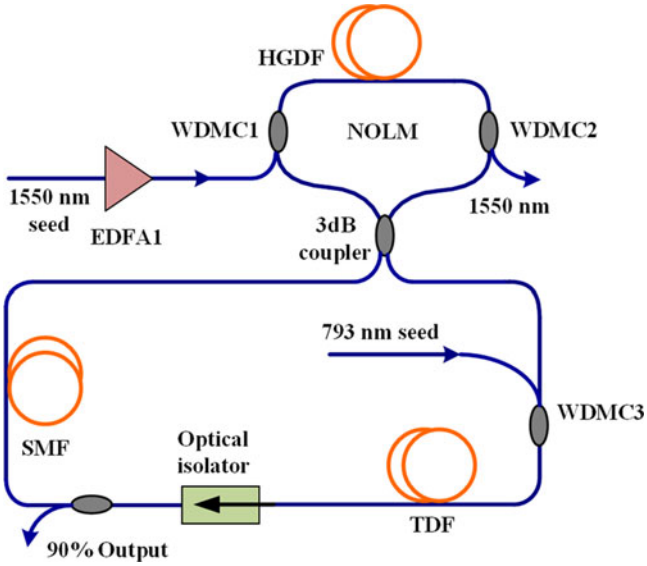

Fig. 3. The structure of the proposed fiber laser.

corresponding full-width at half-maximum (FWHM) wavelength bandwidth, λ is the central wavelength and α denotes the loss in fiber. In particular, g_0 is the saturable gain coefficient of the gain fiber and it is given by

$$g_0 = \frac{g}{1 + P_{av}/P_{sat}} \tag{2}$$

where g is the small signal gain coefficient, P_{av} stands for the average pulse power and P_{sat} is the saturation absorption power.

At the input of the NOLM, the incident light is divided into clockwise wave and counter clockwise wave. The propagation of the pulses in NOLM can be described by the coupled nonlinear Schrodinger equations (NLSE) [24]

$$\frac{\partial A_1}{\partial z} + \frac{i\beta_{21}}{2}\frac{\partial^2 A_1}{\partial t^2} - \frac{\beta_{31}}{6}\frac{\partial^3 A_1}{\partial t^3} + \frac{\alpha_1}{2}A_1 = i\gamma_1|A_1|^2 A_1 + 2i\gamma_{12}|A_2|^2 A_1 \tag{3}$$

$$\frac{\partial A_2}{\partial z} + \frac{i\beta_{22}}{2}\frac{\partial^2 A_2}{\partial t^2} - \frac{\beta_{32}}{6}\frac{\partial^3 A_2}{\partial t^3} + \frac{\alpha_2}{2}A_2 = i\gamma_2|A_2|^2 A_2 + 2i\gamma_{12}|A_1|^2 A_2 \tag{4}$$

where A_1 and A_2 are the slowly varying amplitude at 1.55 μm and 2.053 μm, respectively. β_{2j}, β_{3j} ($j = 1, 2$) are the second- and third-order dispersion coefficients of 1.55 μm and 2.053 μm, respectively. Since the pump and signal are counter- propagation along counter-clockwise direction, the 1.55 μm light is assumed to be a continuous wave with its power equal to the average power of the pump.

4. Simulation Results and Discussion

In this part, we investigate laser performances based on the model as mentioned above. The simulation flow is demonstrated in Fig. 4.

The simulation starts with a Gaussian white noise with total power of 1 mW in the laser cavity. Then it circulates along SMF-NOLM-TDF-OC-SMF. The step length is 0.1 m and the time step is 0.0244 ps. The waveform of the pump light at 1.55 μm is denoted by a hyperbolic secant function with FWHM of 1.8 ps which is close to commercially available laser source at 1.55 μm. The repetition rate is 40 GHz and the peak power is 10 W. The length of SMF, TDF, and HGDF are: $L_{SMF} = 0.5$ m,

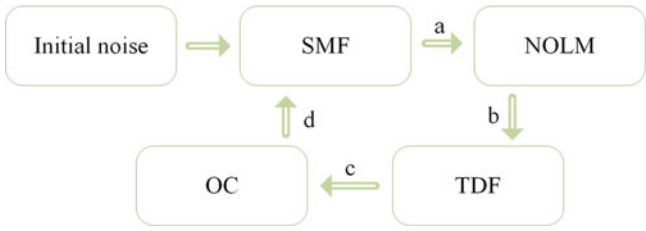

Fig. 4. Flow chart of the simulation process.

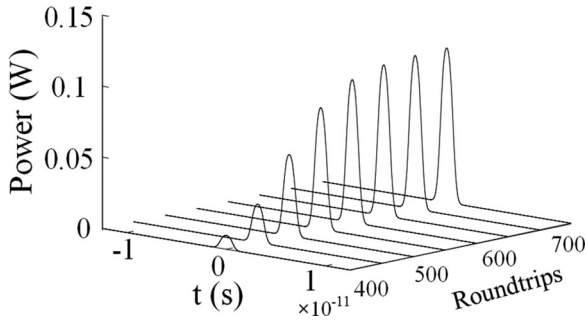

Fig. 5. Result of pulse evolution by every 50 roundtrips.

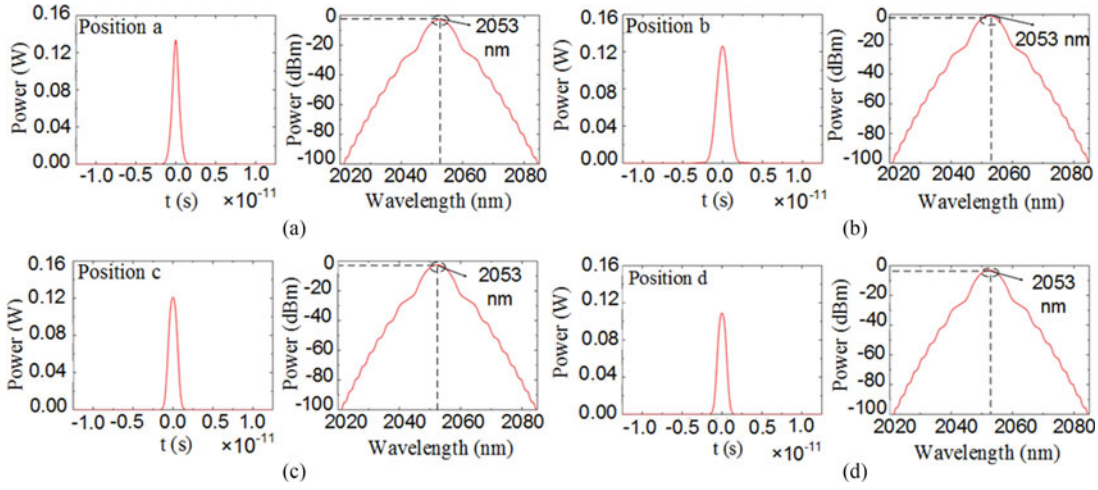

Fig. 6. Output power and spectra at different positions of the cavity.

$L_{TDF} = 1.5$ m, and $L_{GDF} = 4.4$ m, respectively. The second-order dispersion of various fibers are $-0.091\,ps^2/m$, $-0.130\,ps^2/m$, and $0.012855\,ps^2/m$, respectively. Thus the net dispersion in the cavity is $-0.177\,ps^2$. The corresponding nonlinear coefficients are: $\gamma_{SMF} = 1\,W^{-1}km^{-1}$, $\gamma_{TDF} = 3\,W^{-1}km^{-1}$, and $\gamma_{GDF} = 27.3\,W^{-1}km^{-1}$, respectively. The value of g is 0.15 dB/m and $\triangle\lambda$ is equal to 40 nm. Fig. 5 shows the result of the pulse evolution, which was recorded by every 50 roundtrips. Stable optical pulse can be obtained after ~650 roundtrips.

At steady state, the FWHM of the 40-GHz output pulse is 1.29 ps with peak power of 109 mW, indicating the pulse is slightly compressed in comparison with input pump pulse. At steady state, the pulse shape and corresponding spectra at different positions of the cavity are displayed in Fig. 6. The pulse width at positions *a*, *b*, *c*, and *d* are 0.95 ps, 1.79 ps, 1.29 ps, and 1.29 ps, respectively.

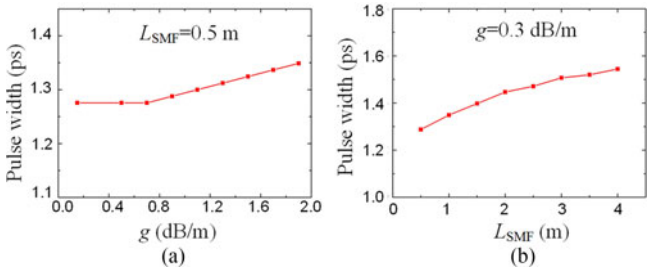

Fig. 7. The width of output pulse (a) and (b) depend on *g* and LSMF, respectively.

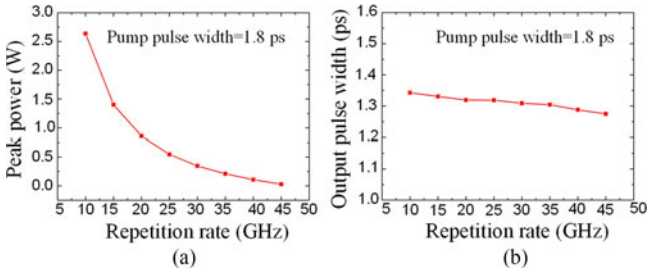

Fig. 8. The peak power (a) and (b) width of output pulse depends on repetition rate.

The pulse broadening from *a* to *b* is due to the negative dispersion in TDF. Since the HGDF shows positive dispersion, the pulse becomes narrower after passing through NOLM. Meanwhile, due to the XPM in HGDF, the chirp is then compensated by the negative dispersion in the following SMF resulting in a pulse width less than 1 ps. The 3-dB bandwidth and 10-dB bandwidth of the spectra are ~6.7 nm and ~11 nm, respectively.

In order to find out the relationships among *g*, L_{SMF} and pulse width, we gradually adjust the values of *g* and L_{SMF}. Fig. 7 shows the variation trend of pulse width. As shown in Fig. 7(a), the pulse width presents an upward trend with increment of *g*. When *g* is smaller than 0.15, no lasing emission is observed since the total loss of the cavity is higher than the gain. As shown in Fig. 7(b), it can be found that the pulse width increases with respect to L_{SMF} because of the net dispersion increment.

One of the advantages of the actively mode-locked laser is that the features of the output pulse can be flexibly adjusted by tuning the pump. With other parameters fixed, the output peak power and output pulse width under different repetition rate are shown in Fig. 8(a) and (b), respectively. It is clearly observed that the output peak power decreases with the increment of repetition rate. This is because as the repetition rate rises up, the mode-locking order increases as well as more pulses are conserved in the laser cavity. These pulses share the total gain provided by the TDF and therefore, the peak power shrinks. To realize even higher repetition rate beyond 100 GHz, higher gain is necessary. In Fig. 8(b), it is found that the output pulse width is compressed slightly in comparison with input pump pulse, and it changes little with different repetition rates.

Next, we change the pump pulse width and investigate its impacts on the 2 μm output. As depicted in Fig. 9 (a), with larger pump pulse width, there is a significant decline of the output peak power since more gain is necessary for a wider pulse to maintain the same peak power. Fig. 9(b) shows the pulse width transfer relation between pump and laser output. The output pulse width can be well manipulated by the pump. This feature is essential in the application of Nyquist pulse shaping [25]. In practice, the pump pulse width can be varied by tunable optical bandpass filtering before optical injection into the laser cavity.

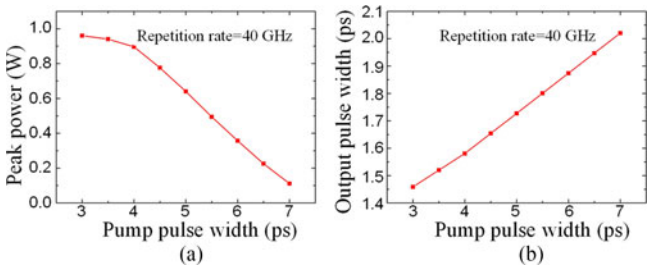

Fig. 9. The peak power (a) and (b) width of output pulse depends on pump pulse width.

5. Conclusion

In summary, an alternative laser configuration for tunable high repetition rate pulse generation at 2 μm is proposed and numerically investigated. In such actively mode-locked fiber laser, inter-band all-optical modulation in a group-velocity- matching HGDF is employed to overcome the challenge of limited operation speed of electro-optical modulators so as to synchronize the 2-μm output by injecting a 1.55-μm pump pulse. Benefitting from the ultrafast response of the nonlinear effect in HGDF, repetition rate higher than 40 GHz can be achieved. Furthermore, the output pulse width can be flexibly adjusted by tuning the pump. For future work, on one hand, photonic crystal fibers with even higher nonlinearity and tailored dispersion can be used to further reduce the cavity length and enhance the modulation efficiency. On the other hand, the cavity dispersion and gain can be optimized to generate various solitons. The proposed laser can find applications including high speed Nyquist pulse shaping and arbitrary waveform generation.

References

[1] K. Yin, B. Zhang, G. Xue, L. Li, and J. Hou, "High-power all-fiber wavelength-tunable thulium doped fiber laser at 2 μm," *Opt. Exp.*, vol. 22, no. 17, pp. 19947–19952, Aug. 2014.
[2] Y. Tang, X. Li, Z. Yan, X. Yu, Y. Zhang, and Q. J. Wang, "50-W 2-μm nanosecond all-fiber-based thulium-doped fiber amplifier," *J. Sel. Topics Quant. Electron.*, vol. 20, no. 5, pp. 537–543, Apr. 2014.
[3] G. Sobon, J. Sotor, I. Pasternak, A. Krajewska, W. Strupinski, and K. M. Abramaski, "260 fs and 1 nJ pulse generation from a compact, mode-locked Tm-doped fiber laser," *Opt. Exp.*, vol. 23, no. 24, pp. 31446–31451, Nov. 2015.
[4] T. Qiao, W. Chen, W. Lin, and Z. Yang, "Generation of Q-switched mode locking controlled rectangular noise-like soliton bunching in a Tm-doped fiber laser," *Opt. Exp.*, vol. 24, no. 16, pp. 18755–18763, Aug. 2016.
[5] Y. Xu *et al.*, "Dissipative soliton resonance in a wavelength-tunable thulium-doped fiber laser with net-normal dispersion," *IEEE Photon. J.*, vol. 7, no. 3, Jun. 2015, Art. no. 1502007.
[6] Z. Li, S. U. Alam, Y. Jung, A. M. Heidt, and D. J. Richardson, "All-fiber, ultra-wideband tunable laser at 2 μm," *Opt. Lett.*, vol. 38, no. 22, pp. 4739–4742, Nov. 2013.
[7] M. Eckerle, C. Kieleck, J. Swiderski, S. D. Jackson, G. Maze, and M. Eichhorn, "Actively Q-switched and mode-locked Tm3+-doped silicate 2 μm fiber laser for supercontinuum generation in fluoride fiber," *Opt. Lett.*, vol. 37, no. 4, pp. 512–514, Feb. 2012.
[8] Z. Y. Yan *et al.*, "Switchable multi-wavelength Tm-doped mode-locked fiber laser," *Opt. Lett.*, vol. 40, no. 9, pp. 1916–1919, May 2015.
[9] T. Y. Huang *et al.*, "All-fiber multiwavelength thulium-doped laser assisted by four-wave mixing in highly germania-doped fiber," *Opt. Exp.*, vol. 23, no. 1, pp. 340–348, Jan. 2015.
[10] H. Zhang *et al.*, "100Gbit/s WDM transmission at 2 μm: Transmission studies in both low-loss hollow core photonic bandgap fiber and solid core fiber," *Opt. Exp.*, vol. 23, no. 4, pp. 4946–4951, Feb. 2015.
[11] M. N. Petrovich *et al.*, "Demonstration of amplified data transmission at 2 microns in a low-loss wide bandwidth hollow core photonic bandgap fiber," *Opt. Exp.*, vol. 21, no. 23, pp. 28559–28569, Nov. 2013.
[12] H. Zhang *et al.*, "Dense WDM transmission at 2 μm enabled by an arrayed waveguide grating," *Opt. Lett.*, vol. 40, no. 14, pp. 3308–3311, Jul. 2015.
[13] T. Hirooka, D. Seya, K. Harako, D. Suzuki, and M. Nakazawa, "Ultrafast Nyquist OTDM demultiplexing using optical Nyquist pulse sampling in an all-optical nonlinear switch," *Opt. Exp.*, vol. 23, no. 16, pp. 20858–20866, Jul. 2015.
[14] Z. X. Zhang, L. Zhan, X. X. Yang, S. Y. Luo, and Y. X. Xia, "Passive harmonically mode-locked erbium-doped fiber laser with scalable repetition rate up to 1.2 GHz," *Laser Phys. Lett.*, vol. 4, no. 8, pp. 592–596, Feb. 2007.
[15] G. Sobon, K. Krzempek, P. Kaczmarek, K. M. Abramski, and M. Nikodem, "10 GHz passive harmonic mode-locking in Er-Yb double-clad fiber laser," *Opt. Commun.*, vol. 284, no. 18, pp. 4203–4206, Aug. 2011.

[16] Q. Jia, T. Wang, W. Ma, Z. Wang, Q. Su, and B. Bo, "Mode-locking thulium-doped fiber laser with 1.78-GHz repetition rate based on combination of nonlinear polarization rotation and semiconductor saturable absorber mirror," *IEEE Photon. J.*, vol. 9, no. 3, Jun. 2017, Art. no. 1502808.
[17] K. Yin, B. Zhang, W. Yang, H. Chen, S. Chen, and J. Hou, "Flexible picosecond thulium-doped fiber laser using the active mode-locking technique, " *Opt. Lett.*, vol. 39, no. 14, pp. 4259–4262, Jul. 2014.
[18] T. Cai and L. R. Chen, "40-80-160 GHz tunable mode-locked semiconductor fiber laser incorporating a nonlinear optical loop mirror," *Opt. Exp.*, vol. 18, no. 17, pp. 18113–18118, Aug. 2010.
[19] E. A. Anashkina, A. V. Andrianov, M. Y. Koptev, V. M. Mashinsky, S. V. Muravyev, and A. V. Kim, "Generating tunable optical pulses over the ultrabroad range of 1.6-2.5 μm in GeO2-doped silica fibers with an Er: Fiber laser source," *Opt. Exp.*, vol. 20, no. 24, pp. 27102–27107, Nov. 2012.
[20] E. A. Anashkina, A. V. Andrianov, M. Yu. Koptev, S. V. Muravyev, and A. V. Kim, "Generating femtosecond optical pulses tunable from 2 to 3 μm with a sililca-based all-fiber laser system," *Opt. Lett.*, vol. 39, no. 10, pp. 2963–2966, May 2014.
[21] E. M. Dianov and V. M. Mashinsky, "Germania-based core optical fibers," *J. Lightw. Technol.*, vol. 23, no. 11, pp. 3500–3508, Nov. 2005.
[22] J. W. Fleming, "Dispersion in GeO2-SiO2 glasses," *Appl. Opt.*, vol. 23, no. 24, pp. 4486–4493, Dec. 1984.
[23] G. P. Agrawal, *Nonlinear Fiber Optics*. New York, NY, USA: Academic, 2007.
[24] B. Crosignani, A. Cutolo, and P. D. Porto, "Coupled-mode theory of nonlinear propagation in multimode and single-mode fibers: Envelope solitons and self-confinement," *J. Opt. Soc. Amer.*, vol. 72, no. 9, pp. 1136–1141, Sep. 1982.
[25] M. Ziyadi *et al.*, "Optical Nyquist channel generation using a comb-based tunable optical tapped-delay-line," *Opt. Lett.*, vol. 39, no. 36, pp. 6585–6588, Dec. 2014.